

Thermal and optical properties of ZTS single crystals in the presence of 1,10-phenanthroline (Phen)

Crystalline perfection studies

S. P. Meenakshisundaram · S. Parthiban ·
R. Kalavathy · G. Madhurambal ·
G. Bhagavannarayana · S. C. Mojumdar

CTAS2009 Special Chapter
© Akadémiai Kiadó, Budapest, Hungary 2010

Abstract The influence of heteroaromatic N-base (1,10-phenanthroline) (Phen), a new additive as complexing agent on tris(thiourea)zinc(II)sulphate (ZTS) crystals from aqueous solutions at 30 °C is investigated. Crystals were grown using low concentration of the dopant (0.005 M L⁻¹) in the aqueous growth medium and the growth promoting effect (GPE) is much greater because of an increase in the metastable zone width. High dopant concentration decreases GPE. The crystalline perfection of the grown crystals is quite good both in doped and undoped crystals as evaluated by high-resolution X-ray diffractometry (HRXRD). The diffraction curve of a typical Phen doped as-grown ZTS crystal was observed to contain a single peak indicating that the crystal does not contain any epitaxial layer on the surface or internal structural grain boundaries. Not much variation is

observed in FT-IR and XRD of pure and doped ZTS. Phen depresses the NLO efficiency of ZTS. It could be ascribed due to the disturbance of charge transfer in the presence of the dopant. The grown crystals were also characterized by UV-Vis, SEM and TG-DTA techniques.

Keywords Characterization · XRD ·
1,10-Phenanthroline · Crystalline perfection ·
Nonlinear optical properties · Thermal analysis

Introduction

Tris(thiourea)zinc(II)sulphate (ZTS) is a good engineering material for device application and laser fusion experiments. It is a novel organometallic crystal with potential application in electro-optic modulation. It belongs to the orthorhombic system with the space group $P_{ca}2_1$ and point group mm2. Although the crystal growth, kinetics and characterization of ZTS have been extensively investigated [1–6], a systematic investigation of the effect of a new organic dopant, Phen on ZTS crystal growth medium has not been reported.

It was observed that organic compounds like ethylenediaminetetraacetic acid (EDTA), urea and thiourea lead to an increase in the growth rate and improvement in quality of different crystals [7]. Likewise, catalytic effect on growth rates is also noticed with inorganic additives like KCl and NH₄Cl [8]. The growth promoting effect (GPE) is due to the complexation of trace metal ion impurities in solution. The resulting complex is not entering into the crystal. Since the complexing agent prevents the entry of impurities into the crystal by complex formation, the growth of the crystal is rapid. Also in the presence of these additives, secondary nucleation is effectively controlled.

S. P. Meenakshisundaram · S. Parthiban · R. Kalavathy
Department of Chemistry, Annamalai University,
Annamalainagar 608 002, India

G. Madhurambal
Department of Chemistry, ADM College for Women,
Nagapattinam, India

G. Bhagavannarayana
Materials Characterization Division, National Physical
Laboratory, Dr. K.S. Krishnan Road, New Delhi 110 012, India

S. C. Mojumdar (✉)
Department of Chemical Engineering and Applied Chemistry,
University of Toronto, Toronto, ON M5S 3E5, Canada
e-mail: mojumdar@unbsj.ca; subhash.mojumdar@utoronto.ca;
scmojumdar@yahoo.com

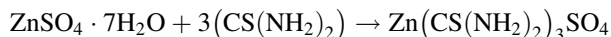
S. C. Mojumdar
Department of Engineering, University of New Brunswick,
Saint John, NB E2L 4L5, Canada

In general, for crystallization to occur, the homogenous phase must be metastable, i.e. supersaturated. An impurity leads to an increase in the metastable zone width of the solution when the complex absorption on the growing surface is not very stable [7]. EDTA, a surfactant is a good additive and the main reason for the rapid growth process in the presence of EDTA is its ability to complex with impurities, particularly the trace metal ions in solution. We have reported [1] that EDTA enhances the second harmonic generation (SHG) efficiency of ZTS remarkably. It will be interesting to carry out the crystal growth and characterization studies in the presence of some other well-known complexing agent to substantiate the above said facts. X-ray, thermal, spectral, microhardness and microscopic studies are very useful techniques for materials characterization. Therefore, it is not surprising that many authors have used these techniques for various materials investigation [9–39]. In this study, we have made a detailed investigation on the influence of complexing agent, a new additive, Phen on ZTS crystals using various spectral, thermal, microhardness, SHG efficiency and microscopic analyses.

Experimental

Synthesis and crystal growth

The starting material was synthesized in the stoichiometric ratio of 1:3 for Zinc Sulphate Heptahydrate (EM) and thiourea (SQ). To avoid decomposition, low temperature (<70 °C) was maintained during the preparation of the solution in deionized water.



The product was purified by repeated recrystallization. The crystal growth was carried out in the presence of a small quantity ($5 \times 10^{-3} \text{ M L}^{-1}$) of organic dopant in the growth medium. At low concentrations of Phen, the GPE is much greater than that observed in the absence of dopant.

The crystal growth was tried under different acidic conditions at pH values in the range of 3.0–6.0. The pH variations were carried out using dilute sulphuric acid. The crystal growth rate and the quality of the crystals are much better when the solution is slightly acidic and the studies were mainly carried out at pH ~5.9. Under high acidity, the rate of crystal growth decreases considerably.

Studies follow the general trend that the growth rate of the crystals in the presence of impurities always decreases with an increase in the impurity concentration. At high concentration of the dopants, the adsorption film blocks the growth surface and inhibits the growth process [40]. Bulk

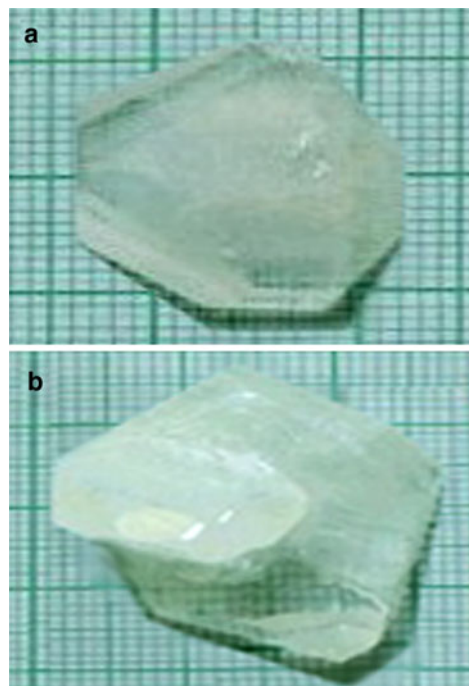


Fig. 1 Photograph of (a) pure ZTS and (b) Phen-doped ZTS

crystals have been grown using the optimized growth parameters. Photographs of the crystals grown from (a) pure ZTS and (b) Phen-doped ZTS solutions are shown in Fig. 1.

Measurements

Powder X-ray diffractometry (XRD) analysis was performed with a graphite monochromated Cu K α radiation.

The FT-IR was recorded for pure ZTS and Phen-doped ZTS using AVATAR 330 FT-IR by KBr pellet technique in the range 500–4000 cm^{-1} .

UV–Visible absorption spectra were recorded using a Hitachi UV–VIS spectrophotometer in the spectral range 250–800 nm.

Thermogravimetric (TG) and differential thermal analysis (DTA) were carried out using a NETZSCH STA 409C thermal analyzer in nitrogen atmosphere. The sample was heated between 30 and 800 °C at a heating rate of 20 °C/min.

Vickers microhardness was evaluated for the well polished grown crystal and dominant (001) plane using Reichert 4000E Ultramicrohardness Tester.

The SEM images were taken at magnification values from 50 \times to 5,000 \times with maximum value of EHT 15.00 kV using a JEOL JSM 5610 LV instrument.

Solubility was analyzed gravimetrically. Metastable zone width was measured by conventional polythermal method [41, 42].

Results and discussion

Solubility and metastable zone width

Metastable zone width is an essential parameter for the growth of large size crystals from solution since it is a direct measure of the stability of the solution in its supersaturated region [43]. Metastable zone width is determined for ZTS/Phen system. Comparison shows that it is wider than in the case of pure ZTS (Table 1). In the present investigations, it is very interesting to note that the metastable zone width increases with increase in temperature for ZTS/Phen system. Also in the presence of Phen, secondary nucleation is controlled to a considerable extent. It effectively depresses the shearing action of the solution tearing off the small particles from crystal surface and thus preventing the secondary nuclei formation.

X-ray diffraction study

XRD pattern of ZTS crystals grown rapidly in $5 \times 10^{-3} \text{ M L}^{-1}$ Phen added solution is compared with that of pure ZTS crystal. X-ray diffraction patterns of the product are consistent with that of the pure ZTS crystal. No change in basic structure is observed except for the slight reduction in intensity with organic dopant (Fig. 2). The XRD data is analyzed with Rietveld method with RIETAN-2000.

FT-IR spectra

The characteristic FT-IR vibrational frequencies of pure ZTS and dopant added ZTS are very similar. The symmetric and asymmetric C=S stretching vibrations at 740 and 1417 cm^{-1} of thiourea are shifted to lower frequencies in all the FT-IR spectra [44]. The band $\sim 1500 \text{ cm}^{-1}$ is assigned to N-C-N stretching vibration. It appears that the GPE of organic dopants is not connected with the additive entering into the crystal. When the impurity distribution coefficient is very low, the impurities are practically not

Table 1 Nucleation temperature and metastable zone width of pure and Phen ($5 \times 10^{-3} \text{ mol/dm}^3$) added ZTS solution at different saturation temperatures

Saturation temperature/ $^{\circ}\text{C}$	Nucleation temperature/ $^{\circ}\text{C}$		Metastable zone width/ $^{\circ}\text{C}$	
	Pure	Phen added	Pure	Phen added
35	32.0	28.5	3.0	6.5
40	34.5	32.0	5.5	8.0
45	38.2	34.5	6.8	10.5
50	43.0	38.5	7.0	11.5

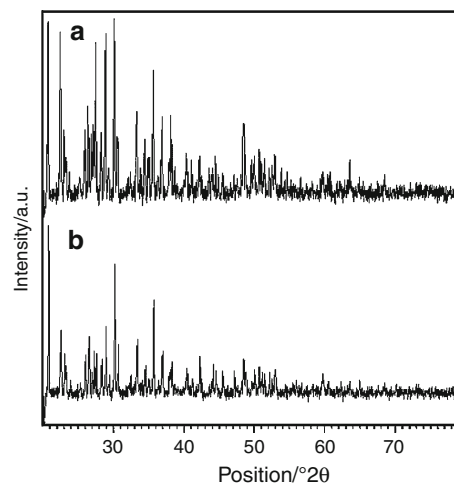


Fig. 2 XRD patterns of (a) pure ZTS and (b) Phen-doped ZTS

incorporated into the crystal [45]. The rapid growth process is caused by the adsorption of the impurity at the flat surface or at the step edge [46]. At low dopant concentrations, adsorption can take place at kink sites (Bliznakov mechanism) or at the surface terrace (Cabrera Vermilyea mechanism). Interestingly at high Phen concentrations, there are some variations in FT-IR spectra [47]. Explanations require a detailed study. The work is in progress.

Optical transmission spectra

The UV-Vis absorption spectra were recorded using a Hitachi UV-Vis spectrophotometer in the spectral range 250–800 nm for pure and Phen-doped ZTS sample. The percentage transmission is much better in the case of Phen doping. The lower cut-off wavelength is $<250 \text{ nm}$.

Microhardness measurements

Hardness is the resistance offered by a material to localized plastic deformation caused by scratching or by indentations.

Microhardness number, $H_V = 1.8544 p/d^2$,

where p is the load in kg and d is the diagonal length of indentation (mm). There is not much of variation in H_V for a test load of 25 g (Table 2).

During indentations, radial cracks have been observed on the prism faces at higher loads ($>30 \text{ g}$).

Thermal studies

The simultaneous TG-DTA curves in nitrogen for ZTS and ZTS/Phen systems at a heating rate of $20 \text{ }^{\circ}\text{C/min}$ are given

Table 2 H_V values

System	Plane	$H_V/\text{kg}/\text{mm}^2$
ZTS	100	120
ZTS/Phen	100	121

H_V value for ZTS taken from Ref. [49]

in the Fig. 3a, b. The absence of water of crystallization in the molecular structure is indicated by the absence of weight loss around 100 °C. Melting point of the sample is slightly lower in the case of Phen added ZTS (Fig. 3b). A very good thermal stability of the material is observed up to ~225 °C and the thermal behaviour is not very much altered in the presence of the dopant, Phen. No decomposition up to the melting point ensures the suitability of the material for application in lasers, where the crystals are required to withstand high temperatures.

Scanning electron microscopic studies

Scanning electron microscopic (SEM) study gives information about the surface nature and its suitability for device fabrication. Also it is used to check the presence of imperfections. It has been reported [48] that the effectiveness of different impurities in changing the surface morphology is different. At low concentrations of dopants the effects are reflected by changes in configuration of grown structures [49]. The SEM pictures of pure and Phen-

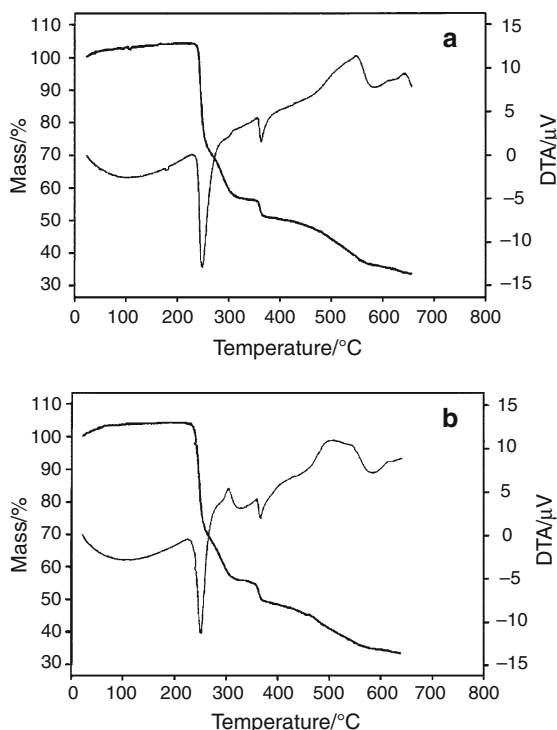


Fig. 3 TG-DTA curve of (a) pure ZTS and (b) Phen-doped ZTS

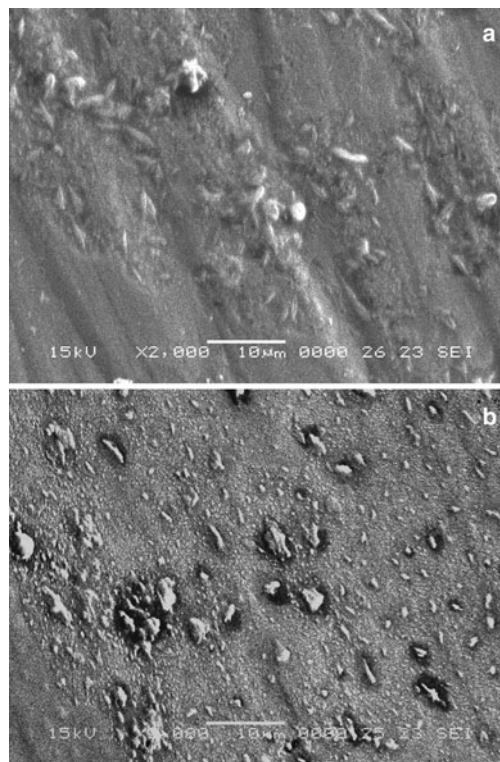


Fig. 4 SEM photograph of (a) pure ZTS and (b) Phen-doped ZTS

doped ZTS are given in Fig. 4a, b. SEM photograph of ZTS (Fig. 4a) shows dendritic growth. Larger scatter centres are observed in Phen-doped ZTS (Fig. 4b). The scatter centre can be understood as a kind of liquid inclusion, mainly mother solution.

High-resolution X-ray diffractometry (HRXRD)

Figure 5a, b shows the high-resolution diffraction curves recorded with the multicrystal X-ray diffractometer [48] in symmetrical Bragg geometry for (001) diffracting planes. A well collimated and monochromated Mo $K\alpha_1$ beam obtained from a set of three plane (111) Si monochromator crystals set in dispersive (+, -, -) configuration has been used as the exploring X-ray beam. Due to this dispersive configuration of the monochromator crystals, the dispersion broadening in the diffraction curve of the specimen crystal is insignificant and the full width at half maximum (FWHM) of the diffraction curve of the specimen does not alter. The specimen crystal is aligned in the (+, -, -, +) configuration. The curves in Fig. 5a, b are having single sharp peaks with FWHM much less than a minute of arc showing good crystalline perfection. The single peak in the curves indicates that the crystal does not contain any epitaxial layer on the surface or internal structural grain boundaries. In general, one can come to a conclusion that the presence of organic dopant improves the crystalline

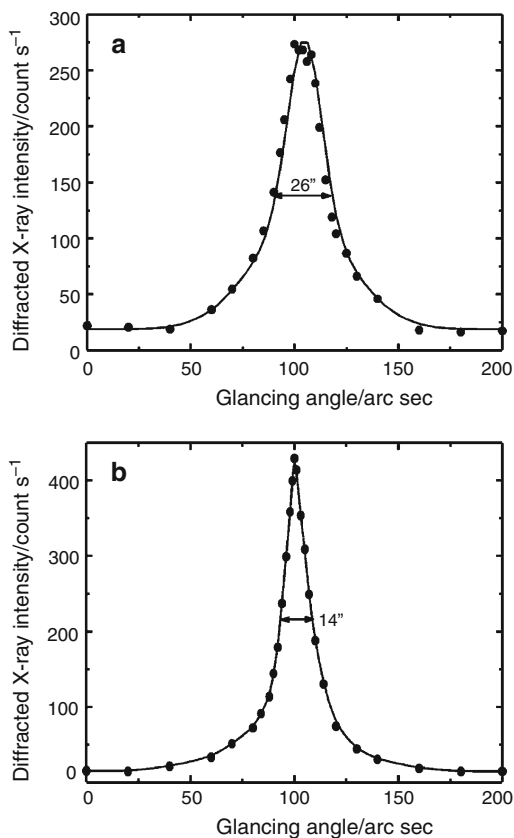


Fig. 5 HRXRD patterns of (a) pure ZTS and (b) Phen-doped ZTS

perfection to a considerable extent as indicated by low FWHM values. High-resolution diffuse X-ray scattering (DXS) studies [50] are in progress to understand the residual point defects and their aggregates in these samples.

SHG efficiency

SHG test on the crystals was performed by Kurtz powder SHG method [51]. The Nd:YAG laser with a modulated radiation of 1,064 nm was used as the optical source and directed on the powdered sample through a filter. The doubling of frequency was confirmed by the green radiation of 532 nm.

Although many materials have been identified that have higher molecular nonlinearities, the attainment of second-order effects requires favourable alignment of the molecule within the crystal structure [52]. To elaborate, the efficient SHG demands specific molecular alignment of the crystal to be achieved facilitating non-linearity in the presence of a dopant. It has been reported that the SHG can be greatly enhanced by altering the molecular alignment through inclusion complexation [53] (Table 3).

Input radiation used is 5 millipoise/pulse. Intensity of SHG gives an indication of NLO efficiency of the material. Depressed SHG output in the case of Phen dopant is quite

Table 3 SHG output

System	$I_{2\omega}/mV$
ZTS	48–49
ZTS/Phen	20–22

likely due to the disturbance of charge transfer. It appears that because of the orientational cancellation, the second order susceptibility for SHG vanishes. By changing the growth conditions and the method, Phen can be an effective dopant. Our belief is based on the fact that the presence of delocalized aromatic organic molecule can result in much higher second order NLO efficiencies.

Conclusions

The metastable zone width of ZTS solutions in their supersaturated region was found to be enhanced by the incorporation of small quantities of 1,10-phenanthroline, a new additive. Phen well promotes the crystal growth process of ZTS in slightly acidic solutions (pH \sim 5.9). XRD and FT-IR studies reveal that the GPE of organic dopant is not caused by adsorption of dopant on the flat surface or the step edge of the crystal. High concentrations of Phen inhibit the growth process. Optical transmission spectral studies reveal that the percentage of transmission is much better with Phen-doped ZTS. Not much variation in microhardness values is observed. HRXRD studies indicate single peak in the diffraction curves of ZTS and ZTS/Phen systems revealing the absence of any epitaxial surface layer or internal structural boundaries that lead to improved crystalline quality. Depressed SHG efficiency with Phen dopant is rationalized by envisaging an unfavourable molecular alignment affecting the nonlinearity.

Acknowledgements We like to thank the Annamalai University and National Physical Laboratory for all the facilities.

References

1. Meenakshisundaram S, Parthiban S, Sarathi N, Kalavathy R, Bhagavannarayana G. Effect of organic dopants on ZTS single crystals. *J Cryst Growth*. 2006;293:376–81.
2. Verma S, Singh MK, Wadhawan VK, Suresh CH. Growth morphology of zinctris(thiourea)sulphate crystals. *J Phys*. 2000;54: 879–88.
3. Gupte SS, Desai CF. Vickers hardness anisotropy and slip system in zinc(tris)thioureasulphate crystals. *Cryst Res Technol*. 1999; 34:1329–32.
4. Venkataramanan V, Dhanaraj G, Wadhawan WK, Sherwood JN, Bhat HL. Crystal growth and defects characterization of zinc-tris(thiourea)sulfate: a novel metalorganic nonlinear optical crystal. *J Cryst Growth*. 1995;154:92–7.

5. Ushasree PM, Muralidharan R, Jayavel R, Ramasamy P. Meta-stable zone width, induction period and interfacial energy of zinctris(thiourea)sulfate. *J Cryst Growth*. 2000;210:741–5.
6. Arunmozhi G, de Gomes EM, Ganesamoorthy S. Growth kinetics of zinc(tris)thioureasulphate (ZTS) crystals. *Cryst Res Technol*. 2004;39:408–13.
7. Sangwal K, Mielniczek-Brzoska E. Effect of impurities on meta-stable zone width for the growth of ammonium oxalate monohydrate crystals from aqueous solutions. *J Cryst Growth*. 2004;267:662–75.
8. Li G, Xue L, Su G, Li Z, Zhuang X, He Y. Rapid growth of KDP crystal from aqueous solutions with additives and its optical studies. *Cryst Res Technol*. 2005;40:867–70.
9. Czakis-Sulikowska D, Czylikowska A, Malinowska A. Thermal and other properties of new 4, 4'-bipyridinetrichloroacetato complexes of Mn(II), Ni(II) and Zn(II). *J Therm Anal Calorim*. 2002;67:667–78.
10. More A, Verenkar VMS, Mojumdar SC. Nickel ferrite nanoparticles synthesis from novel fumarato-hydrazinate precursor. *J Therm Anal Calorim*. 2008;94:63–7.
11. Mojumdar SC, Raki L. Preparation, thermal, spectral and microscopic studies of calcium silicate hydrate-poly(acrylic acid) nanocomposite materials. *J Therm Anal Calorim*. 2006;85:99–105.
12. Sawant SY, Verenkar VMS, Mojumdar SC. Preparation, thermal, XRD, chemical and FT-IR spectral analysis of NiMn₂O₄ nanoparticles and respective precursor. *J Therm Anal Calorim*. 2007;90:669–72.
13. Porob RA, Khan SZ, Mojumdar SC, Verenkar VMS. Synthesis, TG, SDC and infrared spectral study of NiMn₂(C₄H₄O₄)₃·6N₂H₄—a precursor for NiMn₂O₄ nanoparticles. *J Therm Anal Calorim*. 2006;86:605–8.
14. Mojumdar SC, Varshney KG, Agrawal A. Hybrid fibrous ion exchange materials: past, present and future. *Res J Chem Environ*. 2006;10:89–103.
15. Doval M, Palou M, Mojumdar SC. Hydration behaviour of C₂S and C₂AS nanomaterials, synthesized by sol-gel method. *J Therm Anal Calorim*. 2006;86:595–9.
16. Varshney KG, Agrawal A, Mojumdar SC. Pyridine based thorium(IV) phosphate hybrid fibrous ion exchanger: synthesis, characterization and thermal behaviour. *J Therm Anal Calorim*. 2007;90:721–4.
17. Madhurambal G, Ramasamy P, Anbusrinivasan P, Mojumdar SC. Thermal properties, induction period, interfacial energy and nucleation parameters of solution grown benzophenone. *J Therm Anal Calorim*. 2007;90:673–9.
18. Varshney G, Agrawal A, Mojumdar SC. Pyridine based cerium(IV) phosphate hybrid fibrous ion exchanger: Synthesis, characterization and thermal behaviour. *J Therm Anal Calorim*. 2007;90:731–4.
19. Mojumdar SC, Melnik M, Jona E. Thermal and spectral properties of Mg(II) and Cu(II) complexes with heterocyclic N-donor ligands. *J Anal Appl Pyrolysis*. 2000;53:149–60.
20. Borah B, Wood JL. Complex hydrogen bonded cations. The benzimidazole benzimidazolium cation. *Can J Chem*. 1976;50:2470–81.
21. Mojumdar SC, Sain M, Prasad RC, Sun L, Venart JES. Selected thermoanalytical methods and their applications from medicine to construction. *J Therm Anal Calorim*. 2007;60:653–62.
22. Meenakshisundaram SP, Parthiban S, Madhurambal G, Mojumdar SC. Effect of chelating agent (1, 10-phenanthroline) on potassium hydrogen phthalate crystals. *J Therm Anal Calorim*. 2008;94:21–5.
23. Skorsepa JS, Gyoryova K, Melnik M. Preparation, identification and thermal properties of (CH₃CH₂COO)₂Zn·2L·H₂O (L = thiourea, nicotinamide, caffeine or theobromine). *J Therm Anal Calorim*. 1995;44:169–77.
24. Ondrusova D, Jona E, Simon P. Thermal properties of N-ethyl-N-phenyldithiocarbamates and their influence on the kinetics of cure. *J Therm Anal Calorim*. 2002;67:147–52.
25. Kubranova M, Jona E, Rudinska E, Nemcekova K, Ondrusova D, Pajtasova M. Thermal properties of Co-, Ni- and Cu-exchanged montmorillonite with 3-hydroxypyridine. *J Therm Anal Calorim*. 2003;74:251–7.
26. Jona E, Horvath I, Kubranova M, Jorik V. Thermal decomposition reactions of nickel(II) complexes under quasi-equilibrium conditions. II. Study of the relations between thermal, spectral and diffraction properties of the Werner clathrates [Ni(4-Mepy) 4-(NCS)2]·G, (G=benzene, toluene, p-xylene). *J Therm Anal Calorim*. 1993;41:187–96.
27. Czakis-Sulikowska D, Czylikowska A. Complexes of Mn(II), Co(II), Ni(II) and Cu(II) with 4, 4'-bipyridine and dichloroacetates. *J Therm Anal Calorim*. 2003;71:395–405.
28. Verma RK, Verma L, Ranjan M, Verma BP, Mojumdar SC. Thermal analysis of 2-oxocyclopentanedithiocarboxylato complexes of iron(III), copper(II) and zinc(II) containing pyridine or morpholine as the second ligand. *J Therm Anal Calorim*. 2008;94:27–31.
29. Madhurambal G, Ramasamy P, Anbusrinivasan P, Vasudevan G, Kavitha S, Mojumdar SC. Growth and characterization studies of 2-bromo-4'-chloro-acetophenone (BCAP) crystals. *J Therm Anal Calorim*. 2008;94:59–62.
30. Ukraintseva EA, Logvinenko VA, Soldatov DV, Chingina TA. Thermal dissociation processes for clathrates [CuPy₄(NO₃)₂]·2G (G = tetrahydrofurane, chloroform). *J Therm Anal Calorim*. 2004;75:337–45.
31. Mojumdar SC, Melnik M, Jona E. Thermoanalytical investigation of magnesium(II) complexes with pyridine as bio-active ligand. *J Therm Anal Calorim*. 1999;56:541–6.
32. Rathore HS, Varshney G, Mojumdar SC, Saleh MT. Synthesis, characterization and fungicidal activity of zinc diethyldithiocarbamate and phosphate. *J Therm Anal Calorim*. 2007;90:681–6.
33. Mojumdar SC, Madhurambal G, Saleh MT. A study on synthesis and thermal, spectral and biological properties of carboxylato-Mg(II) and carboxylate-Cu(II) complexes with bioactive ligands. *J Therm Anal Calorim*. 2005;81:205–10.
34. Varshney KG, Agrawal A, Mojumdar SC. Pectin based cerium(IV) and thorium(IV) phosphates as novel hybrid fibrous ion exchangers synthesis, characterization and thermal behaviour. *J Therm Anal Calorim*. 2005;81:183–9.
35. Jona E, Rudinska E, Sapietova M, Pajtasova M, Ondrusova D, Jorik V, et al. Interaction of pyridine derivatives into the inter-layer spaces of Cu(II)-montmorillonites. *Res J Chem Environ*. 2005;9:41–3.
36. Mojumdar SC, Miklovic J, Krutosikova A, Valigura D, Stewart JM. Furopyridines and furopyridine-Ni(II) complexes—synthesis, thermal and spectral characterization. *J Therm Anal Calorim*. 2005;81:211–5.
37. Mojumdar SC. Thermal properties, environmental deterioration and applications of macro-defect-free cements. *Res J Chem Environ*. 2005;9:23–7.
38. Madhurambal G, Mojumdar SC, Hariharan S, Ramasamy P. TG, DTC, FT-IR and Raman spectral analysis of Zn₄Mg₆ ammonium sulfate mixed crystals. *J Therm Anal Calorim*. 2004;78:125–33.
39. Mojumdar SC. Thermoanalytical and IR-spectral investigation of Mg(II) complexes with heterocyclic ligands. *J Therm Anal Calorim*. 2001;64:629–36.
40. Kuznetsov VA, Okhrimenko TM, Rak M. Growth promoting effect of organic impurities on growth kinetics of KAP and KDP crystals. *J Cryst Growth*. 1998;193:164–73.
41. Nyvlt J, Rychly R, Gottfried J, Wurzelova J. Metastable zone-width of some aqueous solutions. *J Cryst Growth*. 1970;6:151–62.

42. Zaitseva NP, Rashkovich LN, Bogatyreva SV. Stability of KH_2PO_4 and $\text{K}(\text{H}, \text{D})_2\text{PO}_4$ solutions at fast crystal growth rates. *J Cryst Growth*. 1995;148:276–82.
43. Buckley HE, editor. *Crystal growth*. New York: Wiley; 1951.
44. Silverstein R, Basseler GC, Morrill TC. *Spectroscopic identification of organic compounds*. 5th ed. New York: Wiley; 1998.
45. Rak M, Eremin NN, Eremina TA, Kuznetsov VA, Okhrimenko TM, Furmanova NG, et al. On the mechanism of impurity influence on growth kinetics and surface morphology of KDP crystals-I: defect centers formed by bivalent and trivalent impurity ions incorporated in KDP structure-theoretical study. *J Cryst Growth*. 2005;273:577–85.
46. Eremina TA, Kuznetsov VA, Eremin NN, Okhrimenko TM, Furmanova NG, Efremova EP, et al. On the mechanism of impurity influence on growth kinetics and surface morphology of KDP crystals—II: experimental study of influence of bivalent and trivalent impurity ions on growth kinetics and surface morphology of KDP crystals. *J Cryst Growth*. 2005;273:586–93.
47. Sangwal K. Effects of impurities on crystal growth processes. *Prog Cryst Growth Charact Mater*. 1996;32:3–43.
48. Lal K, Bhagavannarayan G. A high-resolution diffuse X-ray scattering study of defects in dislocation-free silicon crystals growth by the float-zone method and comparison with Czochralski-grown crystals. *J Appl Cryst*. 1989;22:209–15.
49. Ushasree PM, Jayavel R, Ramasamy P. Growth and characterization of phosphate mixed ZTS single crystals. *Mater Sci Eng B*. 1999;65:153–8.
50. Bhagavannarayana G, Choubey A, Shubin YV, Lal K. Study of point defects in as-grown and annealed bismuth germanate single crystals. *J Appl Cryst*. 2005;38:448–54.
51. Kurtz SK, Perry TT. A powder technique for the evaluation of nonlinear optical materials. *J Appl Phys*. 1968;39:3798–813.
52. Hall SR, Kolinsky PV, Jones R, Allen S, Gordon P, Bothwell B, et al. Polymorphism and nonlinear optical activity in organic crystals. *J Cryst Growth*. 1986;79:745–51.
53. Wang Y, Eaton DF. Optically non-linear organic molecules cyclodextrin inclusion complexes. *Chem Phys Lett*. 1985;120:441–4.